Thermal Bubble Formation on Polysilicon Micro Resistors

Liwei Lin[1]
Department of Mechanical Engineering and Applied Mechanics, University of Michigan, Ann Arbor, MI 48109-2125
Mem. ASME

A. P. Pisano

V. P. Carey

Department of Mechanical Engineering, University of California at Berkeley, Berkeley, CA 94720

Thermal bubble formation in the microscale is of importance for both scientific research and practical applications. A bubble generation system that creates individual, spherical vapor bubbles from 2 to 500 μm in diameter is presented. Line shape, polysilicon resistors with a typical size of 50 × 2 × 0.53 μm³ are fabricated by means of micromachining. They function as resistive heaters and generate thermal microbubbles in working liquids such as Fluorinert fluids (inert, dielectric fluids available from the 3M company), water, and methanol. Important experimental phenomena are reported, including Marangoni effects in the microscale; controllability of the size of microbubbles; and bubble nucleation hysteresis. A one-dimensional electrothermal model has been developed and simulated in order to investigate the bubble nucleation phenomena. It is concluded that homogeneous nucleation occurs on the microresistors according to the electrothermal model and experimental measurements.

1 Introduction

The emerging technology of MEMS (microelectromechanical systems) is shrinking mechanical devices into micro and nanometer scales. The trend of miniaturization has brought unprecedented research opportunities in conventional areas of mechanical engineering. Many engineering challenges are expected to be encountered when innovative microdevices are introduced. For example, the commercial success of bubble jet printers (Nielsen, 1985) has inspired many researchers to apply bubble formation mechanism as the operation principle in different microsystems (Zdeblick and Angell, 1987; Sniegowski, 1993; Evans, Liepmann, and Pisano, 1997; Tseng et al., 1996). It is important to study the bubble nucleation and heat transfer processes powered by MEMS microheaters before any of these microdevices may be optimally designed and operated.

This paper addresses bubble nucleation mechanism and heat transfer processes generated by micro-polysilicon line resistors with a typical size of 50 × 2 × 0.53 μm^3. Experiments are recorded under a microscope by passing electrical power through the microresistive heaters while immersing them in subcooled working liquids. Several unprecedented bubble formation phenomena are observed, including stable and controllable bubble sizes during the formation processes and bubble nucleation hysteresis. A one-dimensional electrothermal model is established based on the conservation of energy to help analyzing the heat transfer process. In order to characterize the bubble nucleation mechanism, theories for both heterogeneous and homogeneous nucleation are investigated.

1.1 Previous Works. Boiling phenomenon have been investigated for centuries. Notable experimental investigations may date back to late 1960s. Clark, Strenge, and Westwater (1959) reported that pits with diameters of 0.0003 to 0.003 in. (8 to 76 μm) on a heated surface were active sites for nucleate boiling. Gaertner (1965) later conducted a series of photographic studies and proposed a sequence for nucleate boiling. Other experimental and theoretical studies have followed (Hahne and Grigull, 1977; Stralen and Cole, 1979; Carey, 1992; Stephan, 1992). However, little work can be found in the literature for bubble formation using IC-processed micro resistors.

Several researchers have studied bubble nucleation phenomena by small wire-type heating elements. For example, Pitts and Leppert (1966) used heated wires with a diameter of 0.0005 to 0.051 in. (13 to 1200 μm) in boiling experiments. Sun and Lienhard (1970) investigated the boiling process on horizontal Nichrome cylinders with a diameter of 0.0005 to 0.081 in. (130 to 2060 μm). Bakhru and Lienhard (1972) studied boiling phenomena from small platinum cylinders of 0.001 to 0.004 in. (25 to 102 μm) in diameter. Bubble formation from very short heaters has also been investigated. Baker (1972; 1973) studied the heater length effects for single-phase force convection in pool boiling. Ma and Bergles (1986) used a 1500-μm long heater to study forced boiling convection phenomena. Recently, Lee and Simon (1988) used a 250 × 2000 μm^2 heated patch to study the phase change process in a subcooled, fully developed turbulent flow. Nagasaki et al. (1993) examined the local heating process by using microresistive heaters. All of the above studies contributed different aspects of bubble nucleation processes generated by small heaters. However, these heaters are relatively large when compared with the polysilicon microline resistors presented in this paper.

Analytical theories have also been developed for years to explain the boiling phenomena. For example, Zuber (1961) developed a model for bubble growth in a nonuniform temperature field near a heated surface. Hsu (1962) proposed a model that predicts the size range of active nucleation cavities on a heated surface. Mikic, Rohsenow, and Griffith (1970) established a model for predicting the initial radius of a vapor embryo. All of these models are based on pool boiling conditions for macroscale boiling processes. Therefore, they are generally not applicable for the microscale sub-cooled boiling tests as presented in this paper. Modifications or new theoretical derivations would be required.

2 Experiments

Measurements are performed in a "probe station" apparatus that consists of an optical microscope and several micromanipulators as shown in Fig. 1. Electrical probes are placed right on the contact pads with the help of the micromanipulators. These probes provide electrical interconnections from the power supply and instrument to the microdevices. In order to clearly illustrate the microheater and the two contact pads, Fig. 1 is not drawn to scale. The actual size of the microheater ranges from

[1] Address for correspondence: Department of Mechanical Engineering and Applied Mechanics, University of Michigan, 2350 Hayward Street, Ann Arbor, MI 48109-2121. e-mail: lwlin@engin.umich.edu.

Contributed by the Heat Transfer Division for publication in the JOURNAL OF HEAT TRANSFER. Manuscript received by the Heat Transfer Division, Jan. 6, 1997; revision received, Mar. 6, 1998. Keywords: Bubble Growth, Phase Change, Thermocapillary, Thermophysics, Thin Films. Associate Technical Editor: M. Modest.

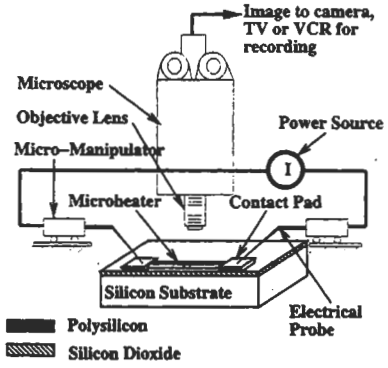

Fig. 1 Schematic drawing of test apparatus

15 to 50 μm in length. The line resistor functions as a resistive heater when an electrical current is applied. Silicon dioxide underneath the resistor is used for electrical and thermal insulation. Silicon substrate, which has a thermal conductivity nearly 100 times higher than that of silicon dioxide, acts as a heat sink.

Two types, standard and irregular, microline resistors have been designed and fabricated. The standard-type resistor has a line shape and its length is 50 $\pm$ 0.1 μm; width is 2 $\pm$ 0.1 μm; and thickness is 0.53 $\pm$ 0.003 μm. The irregular resistor has two different widths, 3 μm (10 μm in length) and 2 μm (5 μm in length), respectively, as shown in Fig. 2. This irregular-shape resistor is designed and fabricated in order to compare and study different thermophysical aspects with respect to the lineshape resistors. Particularly, the thinner portion is expected to endure higher current density such that a higher temperature is expected.

MEMS fabrication technologies are used to fabricate these microdevices. Process details have been described previously (Lin, 1993). Figure 2 shows a scanning electron microscope (SEM) micrograph of a fabricated irregular resistor which is ready for testing. A small beaker is used to hold the working liquid and the fabricated microdevices are immersed at the bottom. The depth of the liquid is about 5 mm. Fluorinert liquids (3M, 1991), DI (Deionized) water, and methanol have been successfully tested as the working liquids to generate thermal bubbles. Although other liquids can certainly be applied, it is noted that if the liquid is not electrically inert, the electrolysis process, instead of thermal bubble formation process, may occur. Therefore, the majority experimental data gathered in this paper are based on the FC liquids which are electrically inert. The experiments are carried out at room temperature and under one atmospheric pressure. Images of the experiments are taken by Polaroid films and recorded on a video tape.

2.1 General Observations. Both a-c and d-c voltage sources have been applied to generate thermal bubbles. The peak values of less than 10 V are found sufficient in bubble formation experiments. Since a small contact resistance exists between the electrical probes and the contact pads, electrical currents, instead of voltages, are measured in major tests to diminish experimental errors. When an a-c source is applied to the microresistor and the driving frequencies are less than 10 Hz, bubbles are formed at twice the signal frequency. It is found that bubble formation does not follow the input frequency greater than about 100 Hz at which the bubble forms and persists. The liquid surrounding the resistor gradually turns into bright color when a d-c input is applied. An individual, spherical shape microbubble is formed when a specific magnitude of input current, "activation current," is applied. After the bubble is nucleated, it grows very quickly until its diameter reaches the length of the resistor. The whole process, including bubble nucleation and growth, takes place in less than one second.

After the initial bubble is formed, three ways of inputing electrical power have been explored. First, the input current is kept at the same level or increased to a higher value than the activation current. The microbubble grows continuously and eventually departs. Second, the current is reduced abruptly after the initial bubble is nucleated. The original bubble is found to collapse and transform into liquid instantly. Third, the input current is reduced gradually after the initiation of bubble formation. In this case, the size of the microbubble will decrease and the bubble stays on the top of the resistor. It is possible to control the bubble size by adjusting the input current. For example, it takes about 10 mW to maintain a stable microbubble on a 50 $\times$ 2 $\times$ 0.53 μm^3 standard resistor in FC 43 liquid. A great portion of this power input actually dissipates down to the substrate. When the input power is further reduced, the size of the bubble continues to diminish. If the bubble is less than 3 μm in diameter, it drifts around the center of the resistor. It is very difficult to control the stability of the bubble at this stage and any reduction of input power will kill the bubble.

These microresistors are very small such that the pool boiling condition has never been established during the experiments. The microresistor creates a local temperature field that may have profound effects to the local flow patterns. For example, the Marangoni effect (Collier, 1981) can be clearly identified which prevents nucleated microbubbles from floating up into the working liquid. In the extreme case, the microbubble tends to stick to the microresistor despite attempts to dislodge it via an electrical probe. Moreover, the bubble may physically move

Nomenclature

A = notation for $(2\sigma_l T_{sat}/h_{lv} d_v)$ in Hsu's analysis
C = constant in Hsu's analysis
d = density, kg m^{-3}
F = thermal conductive shape factor
I = current, Amp
J = current density, Amp m^{-2}
L = length, m
T = temperature, °C
c = specific heat, W m^{-1} °C^{-1}
h_{lv} = latent heat of evaporation, cal kg^{-1}
k = thermal conductivity, W m^{-1} °C^{-1}
R = resistance, ohm
r = cavity radius in Hsu's analysis, m
t = time, s
V = voltage, V
w = width, m
x = coordinate, m
z = thickness, m

Greek Symbols

α = thermal diffusivity, m^2 s^{-1} °C^{-1}
δ = thickness of the limiting thermal layer in Hsu's analysis, m
ϵ = a combined variable in the heat equation, °C m^{-2}
ρ = resistivity, ohm-cm
σ = surface tension, N m^{-1}
θ = temperature difference with respect to bulk, °C
ξ = resistivity coefficient with respect to temperature, °C^{-1}

Subscript

ave = average
c = critical
l = working liquid
o = silicon dioxide
p = polysilicon
ref = reference
s = silicon
sat = saturation
ss = steady state
ts = transient
v = vapor of working liquid
w = wall (surface)
∞ = ambient, bulk

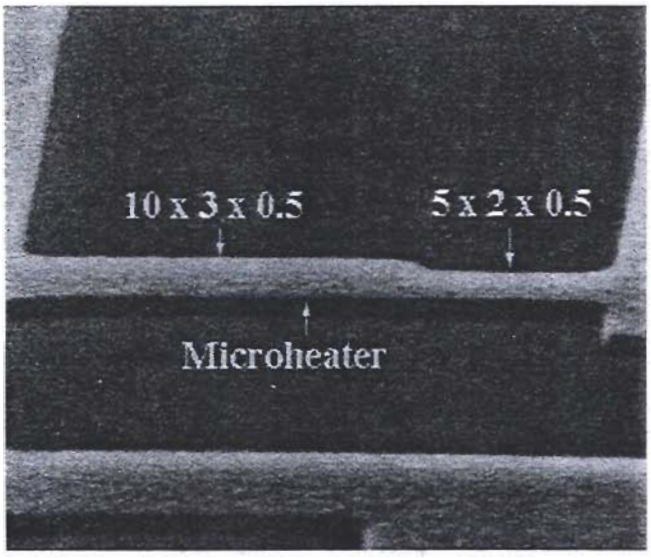

Fig. 2 SEM micrograph of an irregular microresistor

around the substrate by controlling the input current (Lin and Pisano, 1991).

2.2 Bubble Formation on the Irregular Resistor. Experiments on the irregular resistors are conducted and compared with the standard straight-line resistors. Figures 3 to 5 show several steady-state microbubbles generated by the irregular resistor. These experiments are performed in FC 43 liquid and input currents are monitored and recorded. When the input current is less than 12 mA, there is no bubble nucleation. If the input current is larger than 12 mA, a microbubble is nucleated. After bubble nucleation, the input current is reduced to 9.5 mA. A stable microbubble can be maintained as seen in Fig. 3. The two dark objects at both sides of the microphoto are the tips of electrical probes. The microbubble stays at the narrower portion of the resistor and has a diameter of about 2 μm. If the input current is increased, the microbubble grows larger. Figure 4 shows a microbubble with a diameter of 5 μm and the input current is 10 mA. When the input current reaches 12 mA, the size of the microbubble is no longer controllable and the bubble keeps growing. A big microbubble of 500 μm in diameter is seen before detaching in Fig. 5. The objective lens of the microscope has been changed in this photo.

Fig. 4 A microbubble of 5 μm in diameter under a 10 mA input current

3 Electrothermal Modeling

3.1 Thermal Model. The lumped one-dimensional electrothermal model has been derived by the law of energy conservation. A second-order partial differential heat equation can be established as (Lin and Pisano, 1991)

$$\frac{\partial^2 T}{\partial x^2} = \frac{1}{\alpha_p}\frac{\partial T}{\partial t} + \epsilon(T - T_{\text{ref}}) \tag{1}$$

in which T is the temperature along the microline resistor, t is time, and α_p is the thermal diffusivity of polysilicon. Both ϵ and T_{ref} are functions of resistor dimensions and thermal properties. They are summarized below:

$$\alpha_p = \frac{k_p}{c_p d_p} \tag{2}$$

$$\epsilon = \frac{k_o F}{k_p z_p z_o} - \frac{J^2 \rho_p \xi_p}{k_p} \tag{3}$$

$$T_{\text{ref}} = T_\infty + \frac{J^2 \rho_p}{k_p \epsilon}. \tag{4}$$

An excessive shape factor, F, is used to account for the heat conduction losses to the substrate and environment. The shape factor is defined as

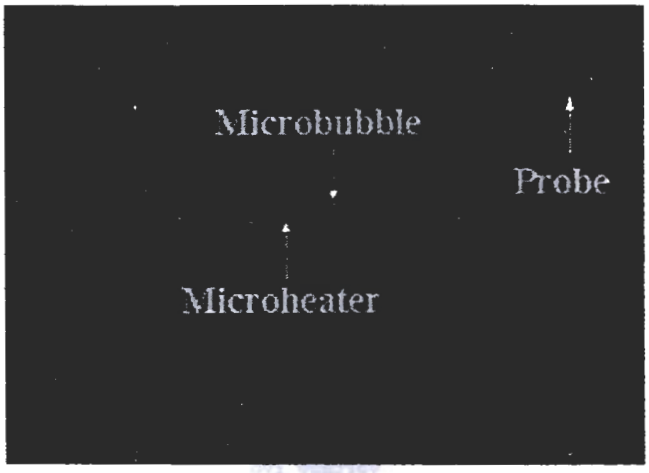

Fig. 3 A single bubble of 2 μm in diameter under a 9.5 mA input current

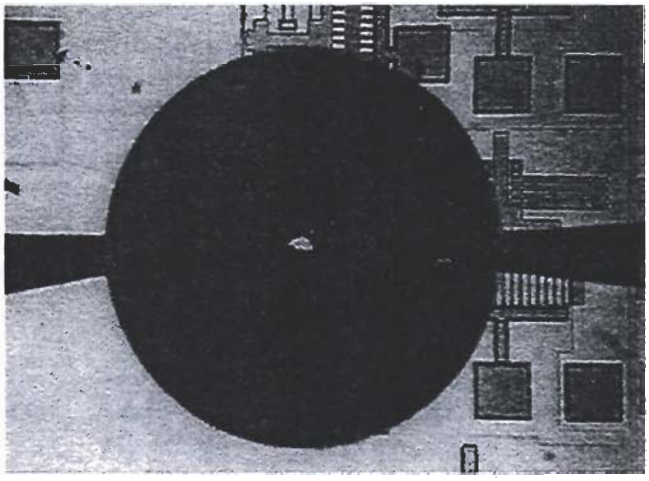

Fig. 5 The final stage of a microthermal bubble before detaching

Table 1 Shape factors for different widths of microresistors in FC43 liquid

Width	Shape Factor
1μm	1.74
2μm	1.30
5μm	1.04

$$F = \frac{\text{total heat flux per unit length}}{\dfrac{wk_o(T - T_\infty)}{z_o}} \tag{5}$$

where the denominator represents the heat flux going directly under the width of the resistor. In order to calculate the shape factor, a two-dimensional finite element simulation has been implemented (Ansoft, 1990). For example, the isotherms around a 2-μm wide microresistor are analyzed and plotted in Fig. 7. The shape factors are calculated accordingly. Some of the numbers with respect to different microresistors are listed in Table 1.

The solutions of Eq. (1) are solved subject to the initial and boundary conditions. It is assumed that the resistor is initially at ambient temperature before heating and both ends of the resistor remain at the ambient temperature. Validation of these assumptions has been proven previously (Lin and Pisano, 1991).

$$T(x = 0, t) = T_\infty \tag{6}$$

$$T(x = L, t) = T_\infty \tag{7}$$

$$T(x, t = 0) = T_\infty \tag{8}$$

The steady-state solution along the micro resistor is derived as

$$T(x)_{ss} = T_{ref} - (T_{ref} - T_\infty)\frac{\cosh\left[\sqrt{\epsilon}\left(x - \dfrac{L}{2}\right)\right]}{\cosh\left(\sqrt{\epsilon}\,\dfrac{L}{2}\right)}. \tag{9}$$

The maximum temperature that occurs at the center of the standard resistor is derived as

$$T(x)_{ssmax} = T_{ref} - (T_{ref} - T_\infty)\frac{1}{\cosh\left(\sqrt{\epsilon}\,\dfrac{L}{2}\right)}. \tag{10}$$

$T(x)_{ssmax}$ depends on ϵ and T_{ref} and both of them are functions of the input current. Therefore, the input current can be measured and used to predict the maximum temperatures on the microline resistor. For irregular-shape resistors, there is no analytical expression for the maximum temperature and numerical analyses are required.

The transient solutions are derived as

$$T(x, t)_{ts} = e^{-\alpha_p \rho^{st}} \sum_{n=1}^{\infty} B_n \sin\left(\frac{n\pi x}{L}\right) e^{-\alpha_p (n\pi t/L)^2} \tag{11}$$

where

$$B_n = \frac{2}{L}\int_0^L [T_\infty - T(x)_{ss}] \sin\left(\frac{n\pi x}{L}\right) dx. \tag{12}$$

It can be observed in the transient solution that the slowest transient decay time ($n = 1$) is in the order of 10 microseconds for a 50-μm long line resistor. For an input source with frequency less than 10 kHz, the temperature of the microline resistor reaches steady state without significant transient delay. This transient decay time can be represented as

$$t_{decay} = \left(\frac{L}{n\pi}\right)^2 \frac{1}{\alpha_p}. \tag{13}$$

3.2 Electrical Model. The electrical model, including voltage and current, can be derived based on the resistance changes with respect to the temperature.

$$R = \int_0^L dR(T) \tag{14}$$

$$= \frac{\rho_p L}{wz_p}(1 + \xi_p(T_{ave} - T_\infty)), \tag{15}$$

where T_{ave} is the average temperature of the line resistor and is expressed as

$$T_{ave} = \frac{1}{L}\int_0^L T dx \tag{16}$$

$$= T_{ref} - (T_{ref} - T_\infty)\frac{\tanh\left(\dfrac{\sqrt{\epsilon}L}{2}\right)}{\dfrac{\sqrt{\epsilon}L}{2}}. \tag{17}$$

Therefore, the voltage across the microline resistor is expressed as

$$V = I\frac{\rho_p L}{wz}(1 + \xi_p(T_{ave} - T_\infty)). \tag{18}$$

This equation is useful to characterize fundamental electrical characteristics of the microline resistors. Figure 6 is the experimental measurements of voltage-current curves for microline resistors. The theoretical predictions as drawn in solid lines are consistent with the experimental data. However, it should be noted that the thermal properties of these thin films are functions of temperature. The above models are only moderately accurate for temperatures less than 300°C which satisfies the operation range of current bubble formation experiments. Modifications are required for high-temperature applications.

3.3 Numerical Simulations. A one-dimensional finite element program, including time responses, has been established to analyze the heat transfer processes of these resistors. This

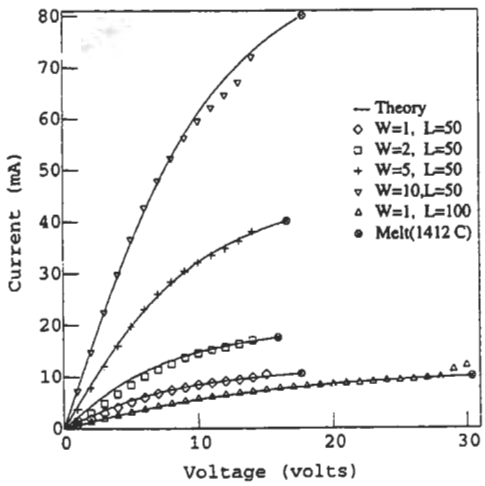

Fig. 6 Comparison between experimental and theoretical *I-V* curves

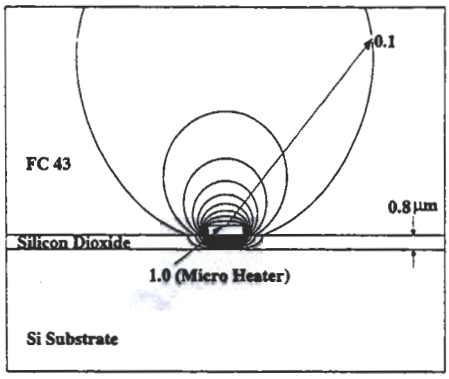

Fig. 7 Cross-sectional view of isotherms around a 2-μm wide microline resistor

finite element model uses 99 nodal points and 49 quadratic elements. It has been built based on Eq. (1) and solved with initial and boundary conditions.

3.3.1 Steady-State and Transient Responses. Figure 8 shows the simulation results of the steady-state temperature profile of a standard line resistor. FC 43 liquid is used in this simulation. It is observed that a relatively uniform, high-temperature region appears at the central region of the line resistor. Moreover, the temperature drops quickly at both ends of the resistor to ambient temperature. The highest current used in this simulation is 11 mA which can create a high temperature of about 300°C. This is a more than enough temperature to nucleate thermal bubbles in most liquids.

The transient analysis is incorporated into the finite element model by using the backward Euler method. Figure 9 is the simulation result that shows the heating process under a step input current of 11 mA. It is observed that steady state is reached in only about 10 microseconds. This number is consistent with the theoretical prediction in Eq. (13). Although 10 microseconds are needed for this microline resistor to reach steady state, only 3 microseconds can bring the resistor temperature over 250°C as shown in this figure.

The cooling process is simulated in Fig. 10. This simulation is conducted by removing the input current of 11 mA. It is noted that only 2 microseconds are needed to cool the resistor to 50°C.

3.3.2 Irregular Microresistor. This finite element model is also used to simulate irregular microresistors. Temperature distributions of the irregular resistor are plotted in Fig. 11. The

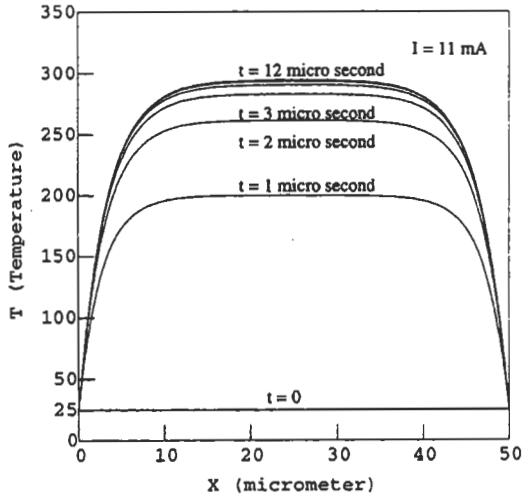

Fig. 9 Heating process of a standard resistor

highest temperature occurs at the narrower portion, 11.6 μm from the left contact pad. This simulation is consistent with the experimental result of Fig. 3, where a microbubble is attached to this hottest spot due to Marangoni effect.

4 Discussions

Experiments, theories, and numerical simulations for bubble formation on microline resistors have been addressed in this paper. They are foundations for characterizing bubble formation on microline resistors. Bubble formation mechanisms and new bubble formation phenomena are discussed in this section based on these analyses and experiments.

4.1 Bubble Formation Mechanisms. Two bubble nucleation mechanisms are examined. For heterogeneous nucleation, bubbles are formed at nucleation sites that are typically provided by surface defects. This type of nucleation can occur for a wide range of superheat temperature. The exact bubble nucleation temperature depends on the size of the cavity and whether vapor is present. Since the microfabrication process is capable of making a very smooth surface, possible surface defects on these microresistors are expected to be extremely small. On the other hand, homogeneous nucleation occurs when liquid approaches the superheated limit such that the liquid phase penetrates the metastable region to a progressively greater degree. In order to

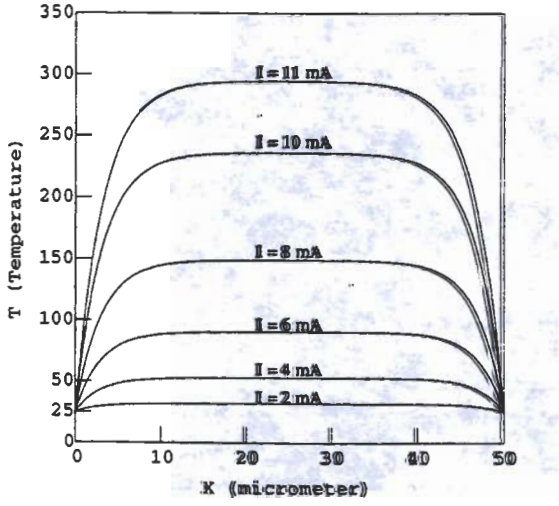

Fig. 8 Steady-state temperature profile of a standard microline resistor

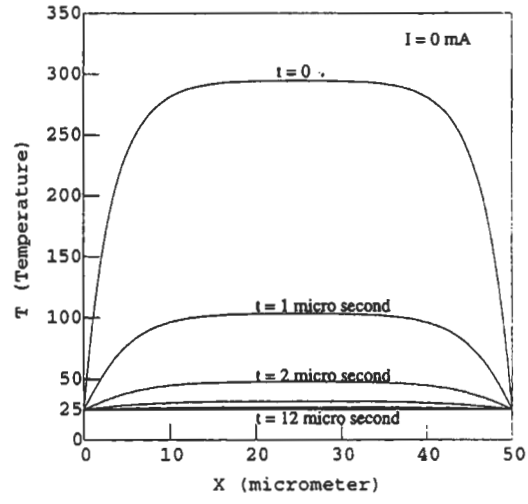

Fig. 10 Cooling process of a standard resistor

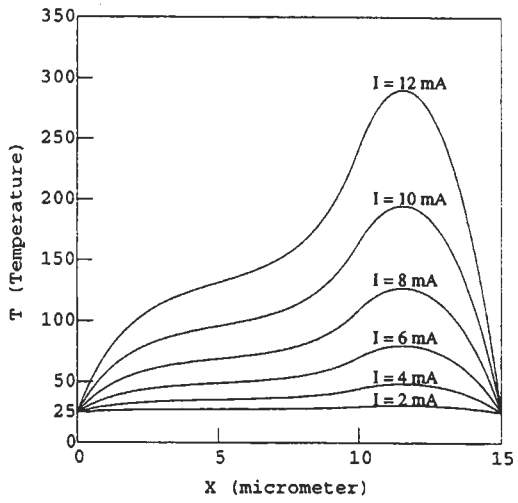

Fig. 11 Temperature distribution of a irregular microresistor

investigate the bubble formation mechanism, the "activation current" is measured. Analytical theories developed in this paper are then used to calculate the bubble nucleation temperatures. Figure 12 shows the experimental results of bubble activation currents and temperatures in three different kinds of Fluorinert liquids (FC 43, FC 75, and FC 72). Microresistors with different widths of 1 to 5 μm and length of 50 μm have been tested. The experimental results suggest that the "activation temperatures" are close to the superheat limits of individual liquids (294°C for FC 43, 227°C for FC 75 and 178°C for FC 72 (3M, 1991)). Similar results are found for DI water and methanol in a previous report that investigated microbubble formation in confined and unconfined microchannels (Lin, Udell, and Pisano, 1993). Both heterogeneous and homogeneous nucleation mechanisms are discussed with the help of these experiments.

4.1.1 Heterogeneous Nucleation. There are several analytical theories that describe the heterogeneous bubble nucleation mechanisms. However, most of these analyses are based on saturated liquid under the pool-boiling condition and they are not directly applicable to the current microboiling experiments. In an effort to address the microscale, subcooled boiling phenomena, a macroscale theory developed by Hsu (1962) is discussed here as the limiting case. According to Hsu's theory,

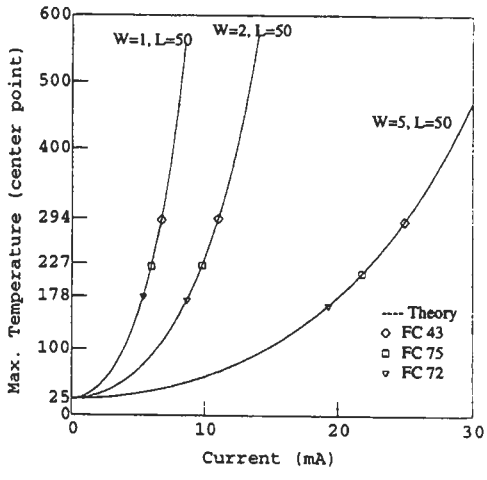

Fig. 12 Experimental results of nucleation currents with respect to temperature

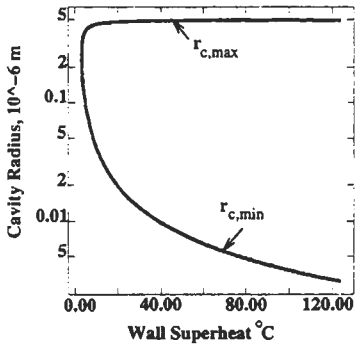

Fig. 13 Range of cavity sizes with respect to superheat temperature based on Hsu's analysis

the effective cavity size for saturated pool-boiling should fall into the following range on a heated surface:

$$r_c = \frac{\delta}{2C_1}\left[1 - \frac{\theta_{sat}}{\theta_w} \pm \sqrt{\left(1 - \frac{\theta_{sat}}{\theta_w}\right)^2 - \frac{4AC_3}{\delta\theta_w}}\right] \quad (19)$$

where A is expressed as the following:

$$A = \frac{2\sigma_l T_{sat}}{h_{\lambda v} d_v}. \quad (20)$$

For simplicity, the cavity mouth is assumed to be a perfect circle and $C_1 = 2$, $C_3 = 1.6$ as described by Hsu (1962). The limiting thermal-layer thickness is estimated to be 1 μm. The surface tension, σ, is estimated to be 2.3 dynes per centimeter according to a previous report that describes microbubble-powered actuators (Lin, Pisano and Lee, 1991). The simulation results are plotted in Fig. 13. It is observed that a superheat temperature of about 20°C is required for bubble nucleation if the cavity is 0.5 μm in radius.

Figure 14 shows the close-view SEM microphoto of a 2-μm wide microline resistor. It is noted that the possible cavities on the surface of the microresistor have a size much less than 0.5 μm in radius. AFM (Atomic Force Microscope) surface analyses are conducted and Fig. 15 shows the scanning result for an area of 0.6 × 0.5 μm^2 on top of the microresistor. The RMS (Root Mean Square) roughness is found to be 6.5 nanometers. A "cavity"-like structure may be identified at the right center of Fig. 15 and a horizontal scan passing through the cavity is drawn at the bottom. The measured peak-to-valley roughness

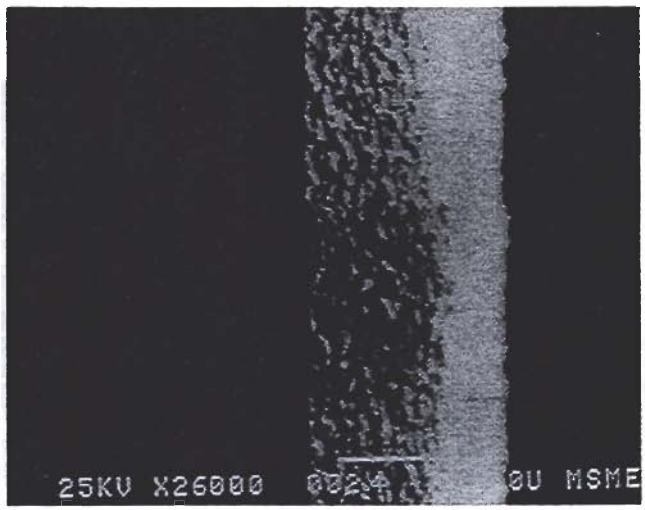

Fig. 14 Close-view SEM photo of a microheater with width of 2 μm

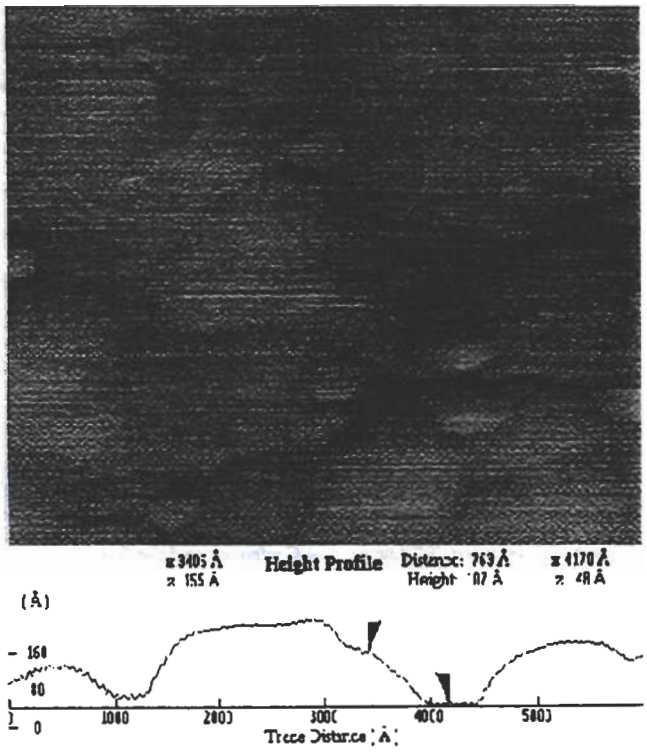

Fig. 15 AFM scanning result on a microresistor

of the cavity is about 10.7 nanometers. If a cavity of this size, 0.01 μm in radius, as suggested by the AFM measurement is actually activated, a superheat temperature of about 80°C should be reached according to Hsu's theory in Fig. 13. However, it should be noted that Hsu's analysis is the limiting case for bubble formation in the microboiling experiments. Further investigations, including modification or derivation of new theories, are required.

4.1.2 Homogeneous Nucleation. Homogeneous nucleation theories with experimental verifications have been derived for many years. There are two spinodal limits, van der Waals spinodal and Berthelot spinodal (Carey, 1992), which predict the thermodynamic limit of superheat. Blander et al. (Blander, Hengstenberg, and Katz, 1971; Blander and Katz, 1975) have demonstrated that the measured superheat limits are higher than the prediction of van der Waals spinodal but lower than that of Berthelot spinodal in their boiling experiments. For the working liquids used in this paper, Table 2 lists the calculation results of both spinodals at one atmospherical pressure. The measured "activation temperatures" as shown in Fig. 12 are clearly close to the superheat limits and spinodals rather than their boiling temperatures. Therefore, the experimental result strongly suggests that homogeneous nucleation occurs on these microline resistors.

4.2 Bubble Formation Phenomena.

4.2.1 Stable and Controllable Bubbles. In pool-boiling experiments, bubble forms and departs. The whole process can be monitored but the reverse of the process, including maintaining a stable bubble or controlling the size of the bubble, is not achievable. Microline resistors provide a unique opportunity to stabilize and control the growing bubble since they can quickly change the temperature field in a confined region. When a microbubble is nucleated, there are two thermal processes that dominate the thermal equilibrium condition: the evaporation process and the condensation process. The evaporation process is related to the input power from the microline resistor. The condensation process is dominated by the liquid/vapor contact interface where vapor is condensed when it meets with cool liquid. In order to reach steady state, these two processes must reach equilibrium. The overall thermodynamic reaction requires complicated three-dimensional analyses, including energy loss to the substrate, the latent heat transfer through the condensation process and simulations for the nonuniform temperature field. A preliminary first-order observation is provided in this paper. According to the energy law, the electrical power is roughly proportional to the square of the input current. On the other hand, the condensation process is roughly dominated by the area of the liquid/vapor interface that is proportional to the square of the bubble diameter. Therefore, under the first-order approximation, the size of the microbubble should change linearly with respect to the input current. Experimentally this trend has been observed (Lin, 1993).

4.2.2 Nucleation Hysteresis. Another important phenomenon to be discussed is the "nucleation hysteresis." The name of nucleation hysteresis follows the report by Bakhru and Lienhard (1972). In Bakhru and Lienhard's experiments, small metal wires (0.001 to 0.004 in. in diameter) were used as the heaters and bubble nucleation tests were conducted in saturated liquids. They found that bubble will nucleate at one temperature, while decrease at a lower temperature. The phenomenon is explained based on macroscale heterogeneous bubble nucleation theories. They suggested that larger nucleation sites are initially filled with liquid and do not function at the beginning of bubble nucleation. Small cavities which are filled with vapor nucleate first at an overshooting temperature. After the initial bubble nucleation, large cavities are filled with vapor and they are functional during the power decreasing process at a lower temperature. Therefore, nucleation hysteresis occurs.

The microscale boiling experiments suggest a different mechanism for nucleation hysteresis. First of all, the cavity theories for pool-boiling experiments are not generally applicable for microboiling experiments as discussed in the previous section. According to the cross-sectional simulation of isotherms as shown in Fig. 7, a thin layer of superheated liquid exists around the microline resistor. When the temperature is high enough such that homogeneous nucleation occurs, the bubble embryo grows with the help of the highly energized, superheated liquid. The stored energy helps the evaporation process during the initiation of the bubble formation and contributes the fast growing of the microbubble as observed in the experiments. After the first stage of bubble formation, the condensation process eventually catches up with the evaporation process as the bubble grows and becomes larger. By lowering the input power, an equilibrium state may be achieved when the evaporation process is in equilibrium with the condensation process. The bubble size becomes controllable at this stage. This explains the reason that the bubble only decreases at a lower temperature which causes nucleation hysteresis.

5 Conclusions

The combination of MEMS technologies and thermal bubble formation provides unique theoretical and experimental challenges. This paper has developed an electrothermal model for microline resistors which can be used as the foundation for further investigations. Experimentally, bubble formation processes are observed and discussed. Based on the established

Table 2 Superheat limits (T/T_c) for FC liquids and water

Liquid	FC 43	FC 72	FC 75	Water
van der Waals	85.5%	85.0%	85.2%	84.5%
Berthelot	92.4%	92.2%	92.3%	91.9%

model and experimental measurements, the bubble "activation temperatures" are close to the critical temperatures of the working liquids. Therefore, it is concluded that homogeneous nucleation occurs on these microline resistors. Several important thermophysical phenomena have been demonstrated:

1 Individual, spherical vapor bubbles with diameters from 2 to 500 μm have been generated by *locally* heating of working fluids.
2 Stable, controllable thermal microbubbles have been demonstrated by microboiling.
3 Strong Marangoni effects have prevented thermal bubbles from floating into working liquids.

Although this paper addresses the fundamentals of bubble formation on microline resistors, many scientific issues and techniques should be further investigated. If clear understanding of boiling phenomena generated by IC-processed microresistors can be achieved, both MEMS fluidic and thermal devices will benefit from these investigations. Specific areas to be explored are: local temperature measurements; models for bubble incipience mechanisms; transport process of vaporization and condensation; and three-dimensional thermal and fluidic models in the microscale.

Acknowledgment

The authors would like to thank Prof. K. S. Udell, Mechanical Engineering Department, U.C. Berkeley for valuable discussions. The devices were fabricated in the U.C. Berkeley Microfabrication Laboratory and this work was supported by Berkeley Sensor and Actuator Center, an NSF/Industry/University Cooperative Research Center. We acknowledge the support by an NSF CAREER Program (ELS-9734421).

References

3M, C., 1991, *Fluorinert Electronic Liquids Product Manual,* 3M Industrial Chemical Production Division, St. Paul, MN.

Ansoft, C., 1990, "Maxwell Solver," 4 Station Square, 660 Commerce Court Building, Pittsburgh, PA, v. 4.33.

Baker, E., 1972, "Liquid Cooling of Microelectronic Devices by Free and Forced Convection," *Microelectronics and Reliability,* Vol. 11, pp. 213–222.

Baker, E., 1973, "Liquid Immersion Cooling of Small Electronic Devices," *Microelectronics and Reliability,* Vol. 12, pp. 163–173.

Bakhru, N., and Lienhard, J., 1972, "Boiling from Small Cylinders," *Int. J. of Heat Mass Transfer,* Vol. 15, pp. 2011–2025.

Blander, M., Hengstenberg, D., and Katz, J. L., 1971, "Bubble Nucleation in *n*-Pentane, *n*-Hexane, *n*-Pentane + Hexadecane Mixtures and Water," *The Journal of Physical Chemistry,* Vol. 75, pp. 3613–3619.

Blander, M., and Katz, J., 1975, "Bubble Nucleation in Liquids," *AIChE Journal,* Vol. 21, pp. 833–848.

Carey, V., 1992, *Liquid-Vapor Phase-Change Phenomena,* Hemisphere Pub. Corp., Washington, DC.

Clark, H., Strenge, P., and Westwater, J., 1959, "Active Sites for Nucleate Boiling," *Chem. Eng. Prog. Symposium,* Vol. 55, pp. 103–110.

Collier, J., 1981, "Convective Boiling and Condensation," 2nd Ed., McGraw-Hill, New York.

Evans, J., Liepmann, D., and Pisano, A. P., 1997, "Planar Laminar Mixer," *Proceedings of IEEE Micro Electro Mechanical Systems (MEMS97),* pp. 96–101.

Gaertner, R., 1965, "Photographic Study of Nucleate Pool Boiling on a Horizontal Surface," ASME JOURNAL OF HEAT TRANSFER, Vol. 87, pp. 17–29.

Hahne, E., and Grigull, U., 1977, *Heat Transfer in Boiling,* Academic Press, New York.

Hsu, Y., 1962, "On the Size Range of Active Nucleation Cavities on a Heating Surface," ASME JOURNAL OF HEAT TRANSFER, Vol. 84C, pp. 207–216.

Lee, T., Simon, T., and Bar-Cohen, A., 1988, "An Investigation of Short Heating Length Effect on Flow Boiling Critical Heat Flux in a Subcooled Turbulent Flow," *Cooling Technology for Electronic Equipment,* Hemisphere, Washington, DC, pp. 435–450.

Lin, Liwei, 1993, "Selective Encapsulations of MEMS: Micro Channels, Needles, Resonators and Electromechanical Filters," Ph.D. dissertation, Mechanical Engineering Department, University of California at Berkeley, Berkeley, CA.

Lin, L., and Pisano, A., 1991, "Bubble Forming on a Micro Line Heater," *Micromechanical Sensors, Actuators and Systems,* ASME, New York, pp. 147–163.

Lin, L., Pisano, A., and Lee, A., 1991, "Microbubble Powered Actuator," *Digest of Transducers '91,* International Conference on Solid-State Sensors and Actuators, pp. 1041–1044.

Lin, L., Udell, K., and Pisano, A., 1993, "Vapor Bubble Formation on a Micro Heater in Confined and Unconfined Micro Channels," *Proceedings of ASME 1993 National Heat Transfer Conference,* ASME, New York, pp. 85–94.

Ma, C.-F., and Bergles, A., 1986, "Jet Impringement Nucleate Boiling," *International J. of Heat and Mass Transfer,* Vol. 29, pp. 1095–1011.

Mikic, B., Rohsenow, W., and Griffith, P., 1970, "On Bubble Growth Rate," *Int. J. Heat Mass Transfer,* Vol. 13, pp. 657–666.

Nielsen, N. J., 1985, "History of Thinkjet Printerhead Development," *HP Journal,* Vol. 36, No. 5, pp. 12–13.

Nagasaki, T., Hijikata, K., et al., 1993, "Boiling Heat Transfer from a Small Heating Element," *Proceedings of the 1993 ASME Winter Annual Meeting,* Vol. HTD-262, pp. 15–22.

Pitts, C., and Lepert, G., 1966, "The Critical Heat Flux for Electrically Heated Wires in Saturated Pool Boiling," *Int. J. Heat Mass Transfer,* Vol. 9, pp. 365–377.

Sniegowski, J., 1993, "A Micro Actuation Mechanism Based on Liquid-Vapor Surface Tension," *Digest of Late News of Transducers '93,* International Conference on Solid-State Sensors and Actuators, pp. 12–13.

Stephan, K., 1992, *Heat Transfer in Condensation and Boiling,* Springer-Verlag, New York.

Stralen, S., and Cole, R., 1979, *Boiling Phenomena: Physicochemical and Engineering Fundamentals and Applications,* Hemisphere, Washington, DC.

Sun, K., and Lienhard, J., 1970, "The Peak Pool Boiling Heat Flux on Horizontal Cylinders," *Int. J. Heat Mass Transfer,* Vol. 13, pp. 1425–1439.

Tseng, F.-G., Linder, C., Kim, C. J., and Ho, C.-M., 1996, "Control of Mixing with Micro Injectors for Combustion Application," *ASME International Mechanical Engineering Congress and Exposition,* Vol. DSC-59, pp. 183–187.

Zdeblick, M. J., and Angell, J. B., 1987, "A Microminiature Electric-to-Fluidic Valve," *Digest of Transducers '87,* International Conference on Solid-State Sensors and Actuators, pp. 827–829.

Zuber, 1961, "Vapor Bubbles in Non-uniform Temperature Field," *Int. J. Heat Mass Transfer,* Vol. 2, p. 83.